Granularity and vortex dynamics in $LaFeAsO_{0.92}F_{0.08}$ probed by harmonics of the ac magnetic susceptibility

Massimiliano Polichetti,[1,2,*] Maria G. Adesso,[1,2] Danilo Zola,[1,2] Jianlin Luo,[3] G. F. Chen,[3] Zheng Li,[3] N. L. Wang,[3] Canio Noce,[1,2] and Sandro Pace[1,2]

[1]*Laboratorio Regionale SuperMat, CNR-INFM, via S. Allende, I-84081 Baronissi (SA), Italy*

[2]*Dipartimento di Fisica "E. R. Caianiello," Universitá di Salerno, via S. Allende, I-84081 Baronissi (SA), Italy*

[3]*Beijing National Laboratory for Condensed Matter Physics, Institute of Physics, Chinese Academy of Sciences, Beijing 100190, China*

(Received 6 August 2008; revised manuscript received 29 November 2008; published 24 December 2008)

Fundamental and higher harmonics of the ac magnetic susceptibility have been measured on $LaFeAsO_{0.92}F_{0.08}$ samples as a function of the temperature, at various amplitudes and frequencies of the ac magnetic field, with a small superimposed dc field parallel to the ac field. The granularity of the samples has been investigated and the intergrain and intragrain contributions have been clearly individuated looking at both the first and the third harmonics. The vortex dynamics has been also analyzed, and a comparison with the magnetic behavior of both the MgB_2 and the cuprate superconductors has been performed. Some vortex dissipative phenomena, i.e., the thermally activated flux flow and the flux creep, have been detected in the presented experimental data, similar to what have been obtained on YBCO. Nevertheless, although the general behavior is similar, several differences have been also evidenced between these different classes of superconductors, mainly in the third harmonics. We infer that different vortex dynamics has to be included into the analysis of the magnetic response in this iron-based material.

DOI: 10.1103/PhysRevB.78.224523 PACS number(s): 74.70.Dd, 74.25.Ha, 74.25.Bt, 74.25.Qt

I. INTRODUCTION

Recently, a relatively high-temperature superconductivity with a critical temperature as high as 26 K, and with an onset temperature at 32 K, has been observed in layered oxypnictide $LaFeAsO_{1-x}F_x$ family,[1] provoking a deep impact in condensed-matter physics community. Indeed, this class of superconductors does not belong to any known categories of high-temperature superconductors such as copper oxide materials,[2] fullerenes,[3] and MgB_2.[4]

Since this family of layered superconductors contains magnetic elements such as Fe or Ni,[5] relevant questions have been raised about the relationship between magnetism and superconductivity, about the origin of the moderately high T_c, and about the chemical and structural parameters that can be used to tune suitable normal-state and superconducting properties. Concerning the iron-based family, the undoped LaFeAsO is a metal, or a degenerate semiconductor at room temperature with no indication of superconductivity, whereas substitution of oxygen with fluorine atoms gives rise to the superconductivity at the F doping of $x=0.03$. Further doping causes a gradual increase in superconducting transition temperature up to the maximum of 26 K for $x=0.11$.[1]

LaFeAsO crystallizes in a tetragonal layered structure of the $P4/nmm$ symmetry[6] (ZrCuSiAs-type structure[7]) made of alternating LaO and FeAs layers stacked along the c axis. The crystal structure is therefore rather simple with a cell containing eight atoms in 2 f.u. and two internal parameters for the position of the La and Fe atoms. The Fe atoms are coordinated by four As atoms in a distorted tetrahedron geometry, two different As-Fe-As bonding angles being observed in the x-ray-diffraction (XRD) experiments. The lanthanum atoms are surrounded by four As atoms and four O atoms in a distorted square antiprism, while the O atoms have four La neighbors arranged in a tetrahedron. Nevertheless, although the crystal structure is substantially different from that of cuprate superconductors, both compounds share intriguing similarities such as (i) the two-dimensional crystal/electronic structure,[8,9] (ii) the presence of a superconducting dome in the electronic phase diagram, where the critical temperature T_c in Fe-based compounds is controlled by a systematic aliovalent ion doping into the insulating block layers,[10] and (iii) a characteristic anomaly in the transport property in the underdoped region.[11]

However, many issues still remain open. Indeed, concerning the superconducting phase, the symmetry of superconducting gap as well as the pairing mechanism is still not known. We also mention that the determination of the actual value of their coherence length is still an open question not excluding that they could be promising for the developments of applications. Moreover, the relevance of spin fluctuations above T_c, the role played by the magnetic rare-earth elements, and the effect of electronic correlations deserve more investigation both theoretically and experimentally. In this respect, these superconductors could offer the possibility to better understand and investigate the mechanisms of the superconductivity in a different context.

As it is well known, in all type-II superconductors a limitation to their specific use is due to the dissipative phenomena associated with the vortex motion inside the sample.[12] Therefore, keeping in mind this consideration, in order to improve both the fabrication process and the application perspectives of these materials, a crucial point is to investigate their flux-pinning and vortex dynamics properties. Among the experimental techniques used in the past to investigate these issues, one of the most efficient is certainly the ac magnetic susceptibility. In this work we report an analysis of the vortex dynamics starting from measurements of funda-

mental and higher harmonics of the ac magnetic susceptibility. This technique has been often used in the past to investigate the superconducting properties,[13,14] and, sometimes, it has been also used to study the pinning properties,[15] the vortex dynamics,[16–20] and the external magnetic field versus temperature (H-T) phase diagram,[21] in several type-II superconductors, both low T_c (Ref. 21) and high T_c,[16,18–20] as well as MgB_2.[19]

The paper is organized as follows. In Sec. II we describe the preparation of $LaFeAsO_{0.92}F_{0.08}$ samples (LaFeAsOF) and illustrate the experimental setup; a motivation of the relevance of the harmonics study is also presented. Then, we discuss the investigation of the temperature dependence of the first and third harmonics of the ac magnetic susceptibility, and the Cole-Cole plots, i.e., the imaginary part of the harmonics as a function of its real part measured at the same temperature T. More specifically, in Sec. III the granularity of the samples has been investigated and a direct comparison with a granular YBCO has also been performed. The vortex dynamics has been investigated in Secs. IV and V, looking at the analysis of the amplitude (Sec. IV) and frequency (Sec. V) dependences of the harmonics of the ac susceptibility. Finally, Sec. VI is devoted to the conclusions.

II. SAMPLE PREPARATION, EXPERIMENTAL SETUP, AND ac MAGNETIC SUSCEPTIBILITY

The polycrystalline samples were prepared by solid-state reaction using LaAs, Fe_2O_3, Fe, and LaF_3 as starting materials. Differently from the synthesis method reported by Kamihara *et al.*,[1] we use Fe_2O_3 as a source of oxygen instead of La_2O_3 due to the high stability of lanthanum oxide. Lanthanum arsenide (LaAs) was obtained by reacting La chips and As pieces at 500 °C for 12 h then at 850 °C for 2 h. Mixtures of four components were ground thoroughly and cold pressed into pellets. The pellets were placed into Ta crucible and sealed in quartz tube under argon atmosphere. Then they were annealed for 50 h at a temperature of 1150 °C. The phase purity was checked by a powder x-ray-diffraction method using Cu $K\alpha$ radiation at room temperature,[10] whereas the composition has also been checked by means of the energy dispersive x-ray spectroscopy (EDS) performed over different areas of the samples. Both structural (XRD) and compositional (EDS) analyses support the good quality of the analyzed specimens.

An extensive scanning tunneling microscopy (SEM) analysis has been performed in order to determine the morphology of our samples. In particular, the images obtained by means of secondary electrons (SEs) and backscattered electrons (BSEs) (not reported here) show a marked granular structure with grains in form of platelets and sticks, with average size of 10 μm, oriented randomly. All the obtained results confirm that the analyzed samples exhibit properties similar to those of other samples known in literature.[22,23]

The first and third harmonics of the ac magnetic susceptibility as a function of the temperature T have been measured on LaFeAsOF bulk samples, by using a Quantum Design PPMS-6000 equipped with an ac susceptometer, at various frequencies ν and amplitudes h_{ac} of the ac magnetic field, in presence of a dc field ($H_{dc}=50$ Oe) parallel to the ac field. Before each measurement, the residual field trapped inside the superconducting dc magnet is reduced to a value $H_{dc}<1$ Oe and the sample is warmed up to a temperature sufficiently higher than the superconducting critical temperature T_c. After that, it is first cooled in zero ac and dc fields down to the starting temperature, remaining about 20 min at that temperature in order to ensure the thermal homogeneity of the sample. We want to notice that the value of the starting temperature depends on the frequency and on the amplitude of the ac field, and on the presence of heating effect, which could produce some consequences on the temperature stability of the sample. Then, the fields are turned on, and all the harmonics data are acquired simultaneously and for increasing temperature, each point being recorded by using a "five-point" measurement mode. By means of this procedure, each single measurement is taken first at the bottom detection coil of the ac susceptometer insert, then at the top detection coil, again at the bottom detection coil, and finally two times at the center of the coil array. In this way, any spurious background signal or effect due to an eventual thermal drift or temperature instability is canceled.

In order to understand the fundamental mechanisms governing the flux lines dynamics of type-II superconductors in the mixed state, their magnetic properties have been extensively studied both using dc and ac magnetic techniques. The results obtained show that the magnetic response of a superconductor could be both linear and nonlinear. The linear case is characterized by the absence of harmonics higher than the first one in the ac magnetic susceptibility. In particular, it is well known that real part of the first harmonic, associated with the screening properties of the sample, is proportional to the time average of the magnetic energy stored in the volume occupied by the sample, whereas the imaginary part is proportional to the energy converted into heat during one cycle of ac field.[13,24] The shape of these two components of the first harmonics as function of the temperature does not substantially change if the external parameters such as the frequency and the amplitude of the ac field or the intensity of an eventual superimposed dc field are changed. It is found that the real part of the susceptibility $\chi_1'(T)$ always shows a steplike transition, corresponding to a behavior characterized by a peak in the imaginary part $\chi_1''(T)$ curve, independently of the experimental parameters that influence the width of the two curves only. Summarizing, from the investigation of the first-harmonic components only, it is not simple to detect the different vortex dynamics regimes governing the ac response of samples in different measurement conditions. On the other hand, when a state with irreversible magnetic properties is present in the material, the current-voltage (I-V) characteristics exhibit a nonlinear behavior. This effect induces the presence of nonlinearities in the magnetic response of the sample which are associated with the appearance of harmonics higher than the first one. On the contrary, the only presence of high-order harmonics does not imply an irreversibility in the magnetic properties of the sample. The physical interpretation given to each of the higher harmonics of the ac susceptibility is still under discussion, as well as the strong differences in the shape of their curves measured in different conditions still need clarifications. Nevertheless, by looking

only at the third harmonics, both experimental and numerical results have shown that, for a sample with given geometry and pinning properties, the shape of the two components $\chi_3'(T)$ and $\chi_3''(T)$ is much more influenced by the presence of particular vortex dynamics regimes.[15,20] So, the higher sensitivity of the third harmonics to the vortex dynamics, together with the opportunity to compare the numerical simulations and the experimentally measured curves, supplies a very powerful tool to extract detailed information about the dynamics regimes governing the ac magnetic response of superconducting samples.

As final consideration, we stress that the plot of the imaginary part as function of the real part of the harmonics (for both the first and the third ones) measured at the same temperature produces the so-called Cole-Cole plot. This kind of representation gives additional information compared to the plot of the separate components as function of the temperature. Indeed, an inspection of these plots allows for a comparison among different samples, and between the experimental data on a sample and the theory, without knowing explicitly the value of the critical current density of the considered samples. Moreover, it gives also the possibility to clearly identify different vortex dynamics regimes. In addition, by using this approach it is possible to distinguish among different models describing a specific flux dynamics regime, which mainly influences the magnetic response of a sample.[25,26]

III. χ_1 AND χ_3: EVIDENCE OF GRANULARITY

Although the granular nature of the transport properties of superconductors can be detected by resistivity measurements,[27] the sensitivity of the ac susceptibility technique allows us to investigate regions of the electrical field, in E-j characteristic, which are not easily detectable by means of the resistivity measurements, especially in bulk samples or powders. Nevertheless, the ac susceptibility measurements have been proved to be a very effective tool to investigate the bulk currents induced in granular superconductors.[28] We also notice that the relatively large dimensions of our samples implies that if the resistivity measurements would be used to analyze their granularity properties, a large amount of current should be needed to obtain accurate results.

A typical behavior of the real and imaginary parts of both the first and third harmonics is shown in Fig. 1, as measured at $\nu=541$ Hz and $h_{ac}=10$ Oe. From these measurements we may infer the granular nature of the samples, and in particular that the contributions at high temperatures correspond to the individual grains of the material which become superconducting (intragranular superconductivity). Practically, the ac magnetic response is determined only by the individual grains which are electrically disconnected from each other. At lower temperatures, corresponding to the intergrain region, the bulk superconductivity becomes relevant. Within this temperature range, the connections between the neighboring grains become superconducting.[29] From Fig. 1, it is possible to clearly distinguish the intergrain and the intragrain contributions. In particular, a double step in the real

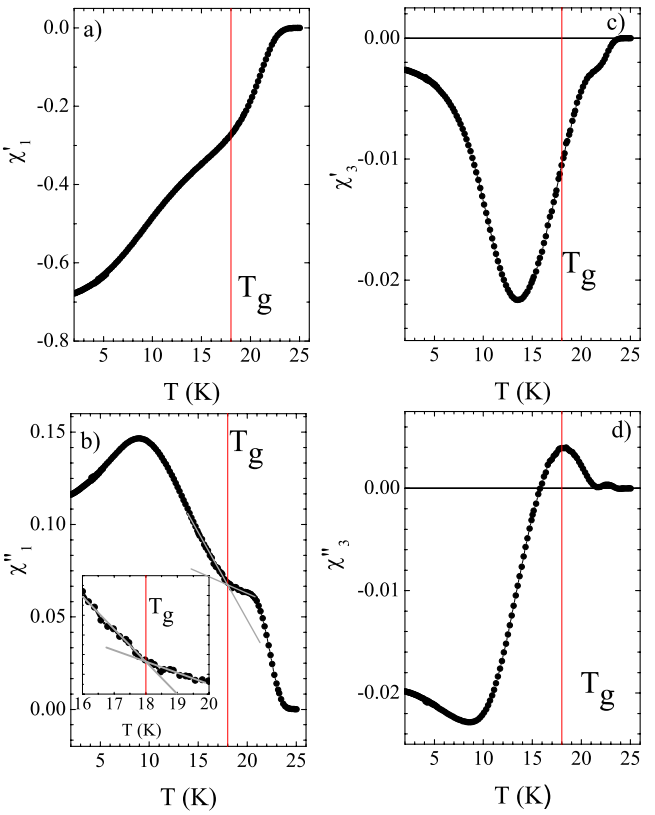

FIG. 1. (Color online) Real and imaginary components of [(a) and (b)] the first and [(c) and (d)] the third harmonics of the ac magnetic susceptibility as functions of the temperature, measured on LaFeAsOF, at $\nu=541$ Hz, $h_{ac}=10$ Oe. The intragrain and the intergrain contributions can be detected. The inset of (b) is a magnification of the area in the $\chi_1''(T)$ around T_g. The straight gray lines, shown in (b) and in the relative inset, are the linear prolongations of the $\chi_1''(T)$ curves after the low-temperature peak and before the high-temperature peak (see text), used to determine the value of T_g.

part of the first harmonics and a double peak in the corresponding imaginary part are known features of a granular magnetic response.[29]

The gray lines, shown in Fig. 1(b) and in the inset of same figure, are the linear extension of the χ'' curves, respectively, after the low-temperature peak and before the high-temperature peak. The intersection of the two lines is used as criterion to determine T_g, i.e., the temperature corresponding to the crossover between a behavior mainly governed by the intergranular component (due to the currents flowing across the grains) and a behavior mainly governed by the intragrain component (due to the currents flowing only inside the grains). The estimated temperature is $T_g=17.8\pm0.4$ K at this amplitude and frequency.

In the corresponding third harmonics (both in the real and in the imaginary parts) it is possible to observe some more complex structures corresponding to the intragrain (near T_c) and the intergrain contributions. In particular, the real part of the third harmonics is characterized by a negative relative minimum (valley) associated with the intragrain component and a negative absolute minimum (peak) at lower temperatures, due to the intergrain currents. Correspondingly, the imaginary part of the third harmonics exhibits a positive

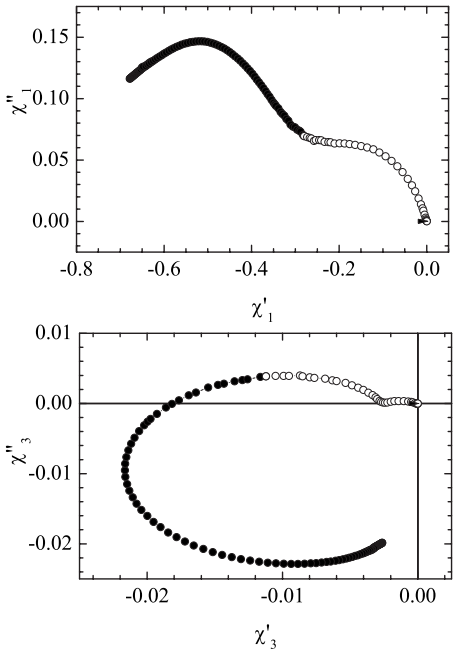

FIG. 2. First- and third-harmonic Cole-Cole plots as measured on LaFeAsOF from 3 to 25 K, at a fixed frequency (ν=541 Hz) and amplitude (h_{ac}=10 Oe) of the ac magnetic field. The two-dome-shaped curve evidences the intergrain and the intragrain contributions. The open symbols indicate the values of the points χ' and χ'' measured above T_g.

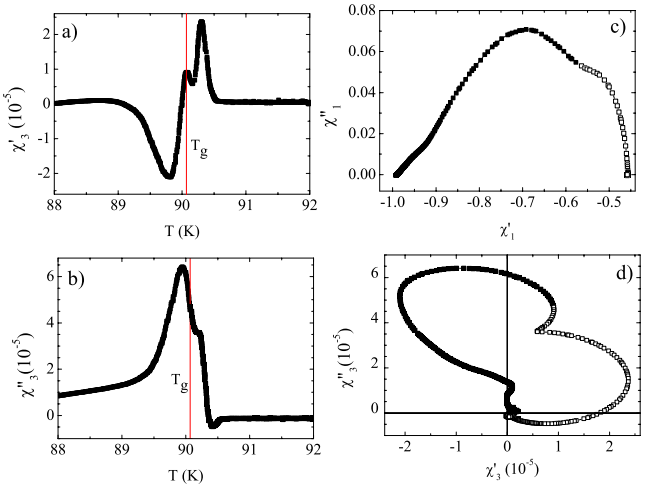

FIG. 3. (Color online) (a) Real and (b) imaginary parts of the third harmonics as a function of the temperature, as measured on a granular YBCO sample, at ν=107 Hz and amplitude h_{ac}=16 Oe. The temperature T_g has been evaluated from the temperature dependence of the first harmonics, not reported here; (c) first- and (d) third-harmonic Cole-Cole plots, obtained on the same sample in the temperature range of 78–95 K, at ν=107 Hz and h_{ac}=16 Oe. Note that the open symbols in the Cole-Cole plots are related to the points (χ',χ'') measured above T_g, and arbitrary units have been used for the susceptibility data.

peak near T_c associated with the intragrain contribution. A further positive peak at lower temperatures is indicative of the crossover from intragrain to intergrain component, its maximum corresponding to the temperature T_g individuated in the first-harmonic measurements. A further negative peak at lower temperatures characterizes the intergrain contribution.

A better way to analyze these two distinct components is by using the Cole-Cole plots, of both the first and third harmonics, i.e., by plotting the imaginary part of each harmonic as a function of its corresponding real part measured at the same temperature. As shown in Fig. 2, the first-harmonic Cole-Cole plot is characterized by a two-dome-shaped curve, corresponding to the intergrain (closed symbols) and to the intragrain (open symbols) contributions, whereas two distinct incomplete loops are associated with the two corresponding magnetic contributions in the third-harmonic Cole-Cole plots.

These features are typical of a type-II granular superconductor. As a comparison, some similar measurements, performed on a commercial YBCO granular sample, are reported in Fig. 3. It is worth pointing out that the behavior of the third harmonic may be discussed only once the intergrain and the intragrain regions of the curves are identified in the first harmonics. A qualitative comparison between the measurements performed on the YBCO and the LaFeAsOF samples suggests that the first-harmonic Cole-Cole plots behave in a similar way in both the superconductors, showing two separate positive peaks, associated with the two contributions. Similar behaviors are also visible in the separated components of the first harmonics, not shown here for the YBCO sample. Although the main structures associated with the granular behavior are evident in both the superconductors, a different shape in the third harmonics has been detected. We would like to point out that the meaning of the peaks and the valleys can be discussed with the help of numerical simulations of the flux dynamic processes governing the ac magnetic response of the sample (see Refs. 15 and 31 for details). From a comparison between the third harmonics of the two superconductors we infer that in the χ_3' curves: (a) the intragrain contribution in the YBCO is characterized by two structures, a positive peak near T_c, followed by a valley at lower temperatures, but still in the positive quadrant, whereas just a negative valley and a further decrease have been detected in the LaFeAsOF measurements; and (b) the intergrain contribution is characterized for both the samples by a negative peak at lower temperatures. On the other hand, in χ_3'' curves there are three main peaks in both the materials: (i) a small peak near T_c in the intragrain component, which is positive in the LaFeAsOF and negative in the YBCO; (ii) a positive peak in both the superconductors, which is associated with the crossover between the intergrain and the intragrain contributions; and (iii) a peak in the intergrain component, which is negative in the LaFeAsOF and positive in the YBCO sample.

Moreover, the third-harmonic Cole-Cole plots are characterized, in both the type-II superconductors, by two separate loops, one associated with the intragrain contribution and the other one with the intergrain contribution. In YBCO we can easily distinguish both the loops whereas in the LaFeAsOF, it is not possible to detect the full intragrain loop. This can be ascribed to the fact that in the latter samples the full Meissner state is not achieved in our measurements. In both the

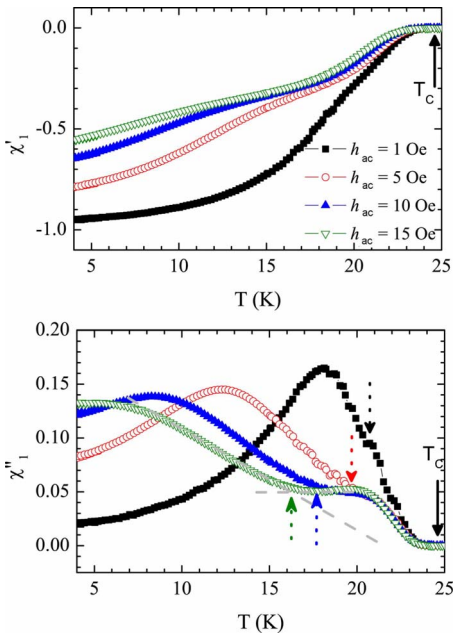

FIG. 4. (Color online) Temperature behavior of the real and imaginary parts of the first harmonics, measured on LaFeAsOF sample at various amplitudes of the ac magnetic susceptibility, at a fixed frequency (ν=107 Hz). The dotted arrows show the T_g temperature evaluated on the different curves by using the criterion described in the text. The value of the critical temperature T_c is also indicated.

samples the intergrain loop is mainly in the left semiplane, but in YBCO it occupies only the positive quadrant, whereas both the positive and the negative ones are occupied by the LaFeAsOF curves. Because of the not completely fulfilled intragrain loop in the LaFeAsOF curves, the main differences between the intragrain contributions of the two superconductors cannot be clearly evidenced. Thus, although several common features between this iron-based superconductor and a granular YBCO sample have been detected, some differences among them have been also evidenced, suggesting that different flux-pinning properties and/or vortex dynamics are dominant in the LaFeAsOF compared to the YBCO.

IV. AMPLITUDE DEPENDENCE OF THE HARMONICS OF THE ac MAGNETIC SUSCEPTIBILITY

In order to analyze the vortex dynamics which mainly influences the magnetic response of this superconductor, measurements at various amplitudes and frequencies of the ac magnetic field have been performed. The present section is devoted to the amplitude dependence of the harmonics, whereas Sec. V will contain the experimental data on the effects of the frequency of ac magnetic field.

In Fig. 4 the real and imaginary parts of the first harmonics, as a function of the temperature, are plotted at various amplitudes of the ac magnetic field, at a fixed frequency (ν =107 Hz). Similar results (not shown here) have been obtained at different frequencies. The height of the negative bump in χ'_1, associated with the crossover between the intergrain and the intragrain components, decreases for increasing h_{ac}. Correspondingly, in the imaginary part of the first harmonics, the height of the peak in the intergrain component slowly decreases with h_{ac}, whereas the peak height due to the intragrain component is characterized by a quick decrease for h_{ac} increasing from 1 to 5 Oe, and an almost constant value for the other amplitudes of the ac magnetic field. We would like also to notice that a critical temperature T_c=24.6 K has been inferred, looking at the first negative χ' point coming out from the noise band, evaluated as large as 10^{-7} emu around zero. Furthermore, we observe that the value here found for T_c is independent of the amplitude of the ac magnetic field. On the contrary, the temperature T_g, indicated in Fig. 4 by the dotted arrows, decreases with a quadratic behavior for increasing h_{ac}, as shown in Fig. 5. For completeness, in this figure the fit parameters are also reported.

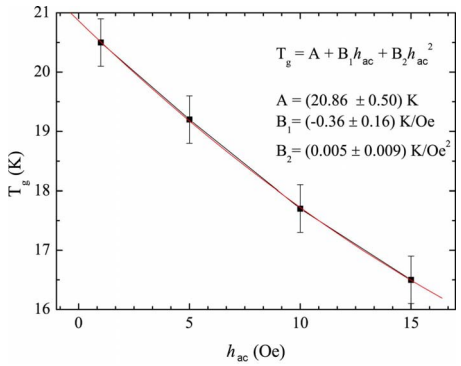

FIG. 5. (Color online) Behavior of T_g as a function of h_{ac}, at fixed frequency ν=107 Hz. The corresponding grain critical temperature T_c is independent of the amplitude of the ac field.

In the first-harmonic Cole-Cole plots reported in Fig. 6 at various amplitudes for given frequencies (107, 541, 1607,

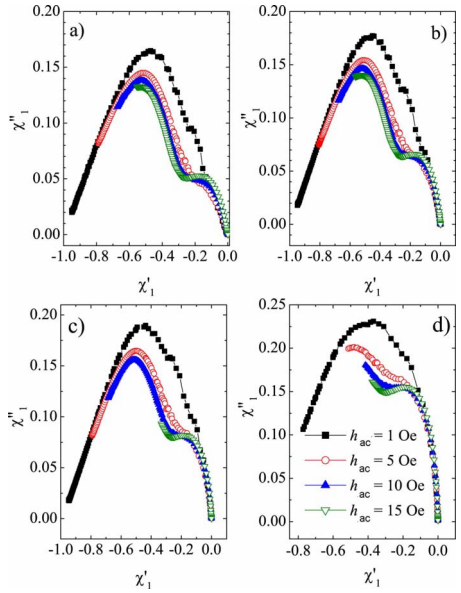

FIG. 6. (Color online) First-harmonic Cole-Cole plots as measured from 3 to 25 K, at various amplitudes of the ac magnetic field and at a fixed frequency: (a) ν=107 Hz, (b) ν=541 Hz, (c) ν =1607 Hz, and (d) ν=9619 Hz.

and 9619 Hz), the maximum in the intergrain components decreases with increasing h_{ac}, for any frequencies chosen. A more complex behavior is observed in the intragrain components, depending on the frequency. These characteristics suggest some indication for the analysis of the experimental curves. In the Bean model,[30] both the first and third harmonics are independent of the amplitude of the ac magnetic field, for any pinning model adopted.[31] Therefore, the observed amplitude dependence in the measured Cole-Cole plots indicates that vortex dissipative phenomena are occurring. In order to investigate the amplitude dependence of the harmonics of the ac magnetic susceptibility in type-II superconductors, some numerical simulations[15–20] have been previously performed, solving the nonlinear diffusion equation of the magnetic field inside the sample (supposing that the sample is an infinite slab), with different *I-V* characteristics, assuming also different pinning[15,16] and flux creep[19,20] models. In all the simulations, a common behavior has been obtained: the first-harmonic Cole-Cole plots are characterized by a dome-shaped curve, whose maximum decreases with increasing h_{ac}.[19] The data obtained here for the intergrain component are in agreement with the previously obtained simulated curves.[15,20] Nevertheless, the behavior of the intergrain contribution, when h_{ac} is varied, is opposite to the experimental results obtained on different type-II superconductors, such as high T_c [YBCO (Ref. 20) and BSCCO (Ref. 29)] and MgB_2.[19] Namely, the first-harmonic Cole-Cole plots in these last materials are characterized by a maximum growing with the amplitude of the ac field. In order to reproduce the experimental results obtained on YBCO and MgB_2, a further dependence on h_{ac} has been included into the pinning potential,[21] whereas the present measurements show that it is not necessary to include this potential to analyze the intergrain behavior obtained on the LaFeAsOF samples. On the other hand, the ac field intragrain response is very similar to that already found on the previously analyzed materials, thus, suggesting that the pinning properties of the LaFeAsOF grains have strong analogies with the properties of MgB_2 and high-T_c materials. Nevertheless, we would like to stress that the analysis of the first harmonics is not enough to identify the vortex dynamics, which may influence the magnetic response of the samples. Indeed, this behavior is common to all the numerical results obtained with different *I-V* curves by using the standard pinning and creep models. Therefore, in order to obtain more insight into this phenomenology it is necessary to analyze the third-harmonic curves.

In Fig. 7, we show the real and imaginary components of the third-harmonic ac susceptibilities, for the same choice of the parameters adopted for the first-harmonic curves reported in Fig. 4. A first rough comparison between Figs. 7 and 4 indicates that the granularity features can be distinguished also in the third-harmonic components. A more detailed inspection at both the first- and the third-harmonic components reveals the presence of different onset temperatures (see Fig. 8), namely, T_c=24.6 K for the first and $T^\star$=23.9 K for the third harmonics. Furthermore, these onset temperatures are independent of the amplitude of the ac magnetic field. This temperature difference between $T^\star$ and T_c is indicative that a dissipative linear phenomenon is occurring in the temperature range $[T^\star, T_c]$, assuming that the harmonics higher than

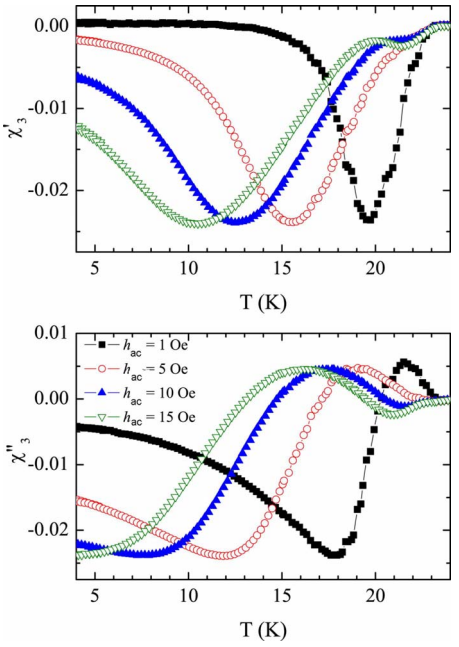

FIG. 7. (Color online) The real and imaginary parts of the third harmonics as a function of the temperature, as measured at various h_{ac} at a fixed frequency (ν=107 Hz).

the third ones are negligible with respect to the third ones. Both the flux flow (FF) and the thermally activated flux flow (TAFF) are nonlinear dissipative phenomena, in absence of a dc field. Nevertheless, with a dc magnetic field higher than the ac one the field dependence of the FF and of the TAFF resistances disappears, generating a linear diffusion process of the magnetic field so that no higher harmonics contribution is expected. Some numerical results previously obtained[32] show that in the presence of a dc magnetic field, a characteristic temperature may be identified such that above it the harmonics behavior is governed by the linear TAFF resistance. This temperature is approximately coincident with the onset temperature of the third harmonics. Therefore, a difference ΔT_{on} between $T^\star$ and T_c represents the experimental evidence of the presence of linear TAFF phenomena

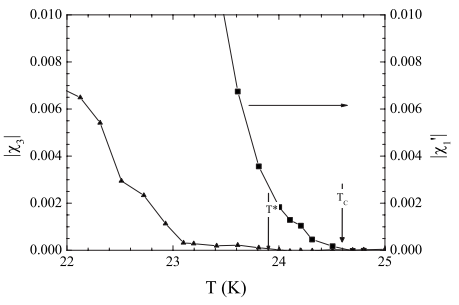

FIG. 8. Magnification of the temperature region around the transition, showing the difference between the onset temperatures of the real part of the first harmonics (indicated with T_c) and of the module of the third-harmonic (indicated with $T^\star$) curves as function of T. In particular these curves are measured at ν=107 Hz and h_{ac} =1 Oe, H_{dc}=50 Oe, and the difference $[T_c - T^\star]$ does not depend on the amplitude of the ac magnetic field.

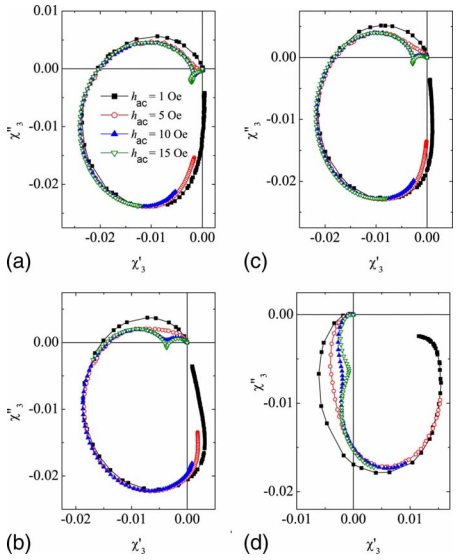

FIG. 9. (Color online) Third-harmonic Cole-Cole plots as measured from 3 to 25 K, at various amplitudes of the ac magnetic field and at a fixed frequency: (a) ν=107 Hz, (b) ν=541 Hz, (c) ν =1607 Hz, and (d) ν=9619 Hz.

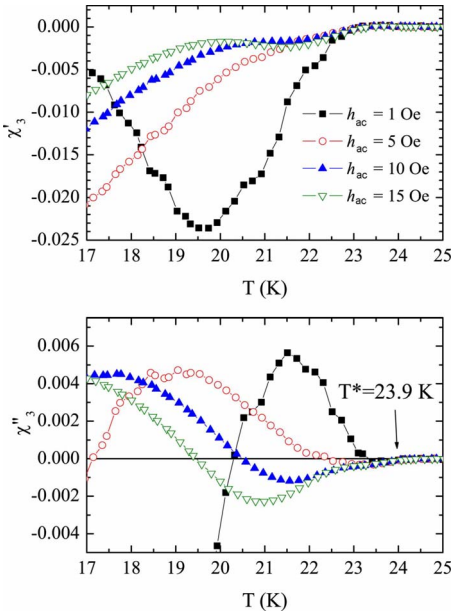

FIG. 10. (Color online) Enlargement of Fig. 7 in the temperature window corresponding to the intragrain contribution.

in the system under analysis. A similar result was also obtained for YBCO bulk samples.[16] From an analysis of the third-harmonic curves, we observe that both in their real and imaginary part (see Fig. 7), the negative peaks in the intergrain region become wider by increasing h_{ac}, although their heights (in absolute value) stay almost constant. This ac field independence of the peak heights is even more evident if we look at the intergrain loops in the third harmonics Cole-Cole plots, as shown in Fig. 9. These curves have been obtained varying the amplitudes (1, 5, 10, and 15 Oe) and frequencies (107, 541, 1607, and 9619 Hz) of the ac field.

The presence of the intergrain negative peak in the real part of the third harmonics, at a temperature lower than that where the peak in the imaginary part of the first harmonics appears, indicates the existence of a pronounced flux creep governing the bulk magnetic response of our samples, similar to what happens in measurements previously performed on YBCO samples.[16] The behavior of the intragrain component as function of h_{ac} reported in Fig. 10 shows that the real part of the third harmonics maintains its general shape, both the relative and the absolute minima moving toward lower temperatures for increasing amplitudes. This behavior indicates that, at least for the used ac field range, no modification of the vortex dynamics regime is produced. In the imaginary part χ''_3, the positive peak tends to become wider and to move toward lower temperatures, whereas a negative peak near T_c tends to become more evident at higher h_{ac}, in agreement with the results obtained for YBCO samples.

V. FREQUENCY DEPENDENCE OF THE HARMONICS OF THE ac MAGNETIC SUSCEPTIBILITY

In Fig. 11 both the real and the imaginary parts of the first harmonics as a function of the temperature are shown, at various frequencies for a fixed amplitude (h_{ac}=1 Oe) of the ac magnetic field. Looking at this figure, we observe that the curves depend on the frequency only in the temperature range of 9–24 K, and the critical temperature T_c is still 24.6 K, independently of the frequency. Moreover, the temperature T_g, again individuated with the same criterion discussed previously, is independent of the frequency within the experimental errors (T_g=20.5 ± 0.4 K), and this behavior is even more evident if the amplitude of the ac field is increased. Nevertheless, both in the intergrain and in the intra-

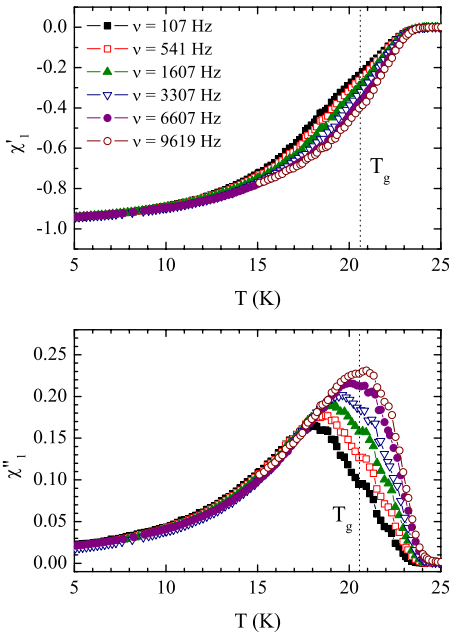

FIG. 11. (Color online) Temperature behavior of the first harmonics of the ac magnetic susceptibility for a fixed amplitude (h_{ac}=1 Oe) at various frequencies of the ac magnetic field. The dotted line identifies the temperature T_g in all the curves.

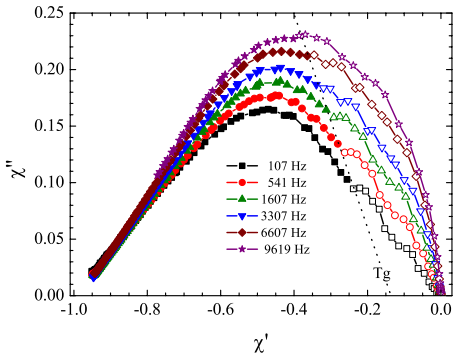

FIG. 12. (Color online) First-harmonic Cole-Cole plots, as measured from 3 to 25 K, at various frequencies of the ac magnetic field and at $h_{ac}=1$ Oe. The open symbols are the (χ',χ'') points measured above T_g, which is represented by the isothermal dotted line in the figure

grain components, a similar behavior with the frequency can be deduced. In particular both the peaks in the imaginary part of the first harmonics, associated with the intergrain and the intragrain contributions, shift toward higher temperatures with a growing height for increasing frequencies. This common behavior in the intergrain and the intragrain first-harmonic components with the frequency of the ac magnetic field is representative that a vortex dynamical phenomenon with a similar frequency dependence is occurring both inside and outside the grains. This is also supported by the first-harmonic Cole-Cole plots shown in Fig. 12, where the intergrain and the intragrain contributions can be separately observed: in both these contributions, the peak height of the dome-shaped curves grows for increasing frequencies.

A growing height with the frequency both in the peak of the imaginary part of the first harmonics and in the maximum of the first-harmonic Cole-Cole plots is indicative of a vortex glass phase, characterized by a collective flux creep,[33] being this behavior opposite to that in the curves simulated by using the Kim-Anderson flux creep model.[33] Nevertheless, for a clear identification of the vortex glass phase, it is also necessary to perform the analysis of the third-harmonic curves, which in our case results in a quite complex task. In Fig. 13, the real and the imaginary parts of the third harmonics are shown at various frequencies. An enlargement of Fig. 13 on the intragrain component is reported in Fig. 14. The corresponding third-harmonic Cole-Cole plots are reported in Fig. 15. The real part of the third harmonics (see Fig. 13) is characterized by two peaks, corresponding to the intergrain and the intragrain contributions. The intergrain part of the curves exhibits a negative peak at lower frequencies. For higher frequencies the peak height (in the absolute value) decreases and a positive peak appears at frequencies higher than 1600 Hz. Nevertheless, in the intragrain real part of the third harmonics (shown in Fig. 14) no changes in the general shape are present, being this shape characterized by a negative peak with a minimum height which decreases for increasing frequencies.

On the contrary, in the imaginary part of the third harmonics, the intergrain component has always the same shape, with a minimum height decreasing for growing ν, whereas

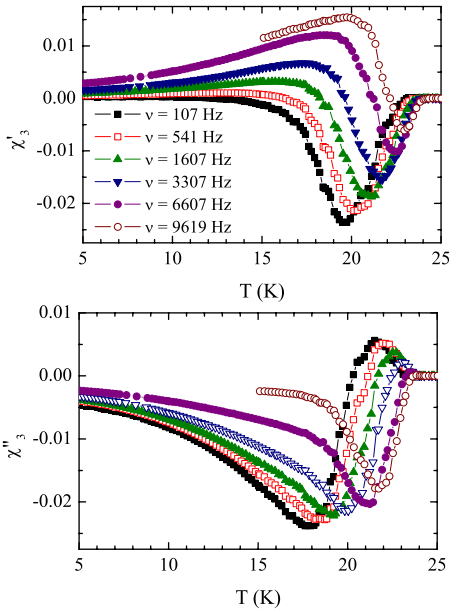

FIG. 13. (Color online) Temperature behavior of the real and imaginary parts of the third harmonics measured at various frequencies of the ac field at fixed $h_{ac}=1$ Oe.

the intragrain behavior, shown in Fig. 14, is characterized by a modification of the shape of the curves. Namely, for increasing frequencies the positive peak near T_c decreases, changing its temperature; then it becomes a negative relative minimum, and finally merges into the intergrain contribution. By taking into account both the frequency and amplitude dependences of the harmonics, we conclude that the vortices moving inside the grains react to the application of the ac field in different dynamical ways with respect to those moving across the grains. Finally, the third-harmonic Cole-Cole plots (Fig. 15) are almost completely in the left half plane at the lowest frequency (107 Hz). For increasing frequencies, they tend to the right half plane and their area decreases. We

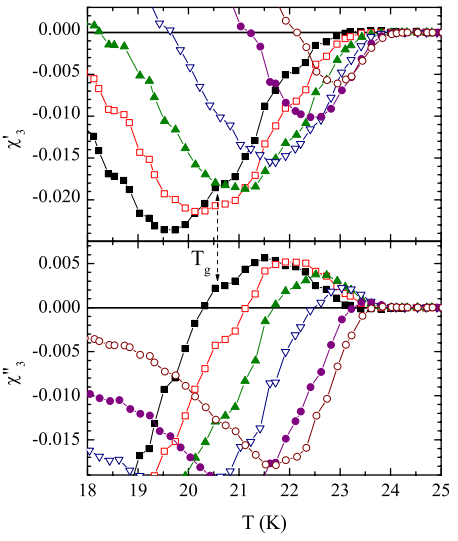

FIG. 14. (Color online) A magnification of Fig. 13 in a window where the intragrain behavior can be easily seen. The arrow across the two plots indicates the temperature T_g.

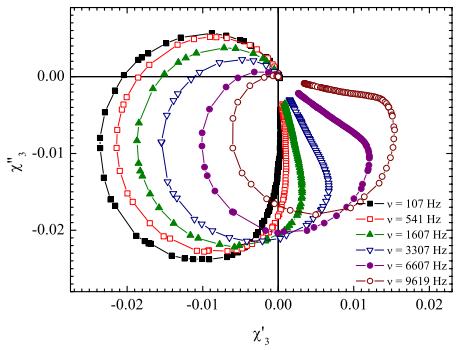

FIG. 15. (Color online) Third-harmonic Cole-Cole plots, as measured from 3 K to 25 K, at various frequencies of the ac magnetic field and at $h_{ac}=1$ Oe.

would like to notice that the curves at high frequencies correspond to a tendency toward the Bean curves, which are closed loops all staying in the right half plane. These behaviors cannot be interpreted in terms of a standard vortex glass phase and are also opposite to the measured YBCO third-harmonic Cole-Cole plots,[33] which, on the contrary, tend to occupy the left half plane for increasing frequencies, with an almost constant area.

VI. CONCLUSIONS

The first and third harmonics of the ac magnetic susceptibility have been measured on LaFeAsOF granular samples as functions of the temperature, at various amplitudes and frequencies of the ac applied magnetic field. A detailed comparison between the obtained results and the magnetic behavior of the cuprate superconductors, as well as the MgB_2, has been performed. Some fundamental differences have been revealed between the magnetic response of LaFeAsOF when compared to the above-mentioned superconductors, and they can be mainly ascribed to different flux-pinning and/or vortex dynamical properties. In particular, the different dependence on the ac field amplitude in the intergrain component of the first-harmonic Cole-Cole plots implies that the standard pinning and flux creep are appropriate enough to analyze the ac magnetic response coming from the bulk currents flowing across the grains in this iron-based material. On the other side, a further amplitude dependence has to be included in the pinning potential to interpret the curves related to the ac magnetic response of the separated grains.

The dissipative phenomena due to the vortex motion have been also investigated. In particular, by the experimental observation of different onset temperatures in the first and third harmonics, the linear TAFF has been detected. Moreover, a combined analysis of the first and the third harmonics allows for the identification of the nonlinear flux creep in the intergrain component. The frequency dependence observed in the imaginary part of the first harmonics, as a function of the temperature, as well as in the corresponding first-harmonic Cole-Cole plots may give some indication about the existence of a vortex glass phase.

The difficulties of detecting a vortex dynamical regime, which may influence the full magnetic response of the analyzed superconductor, are mainly due to the granular nature of the samples. In particular, the analysis of the amplitude and frequency dependences in the intergrain and intragrain components shows that the vortex dynamics occurring inside the grains is different from that produced between the grains. Moreover, a shape change in the imaginary part of the third harmonics in the intragrain component, both with the amplitude and the frequency of the ac magnetic field, together with a shape modification of the real part of the third harmonics with the frequency in the intergrain component, is indicative that the vortex dynamics is changing with the external parameters. This last consideration suggests that the experimental data cannot be reproduced by numerical simulations obtained using the same flux creep model in all the curves, but a more complex analysis is needed to individuate the suitable model to be used when different external magnetic conditions are involved.

Finally it is worth underlying that a preliminary analysis, similar to the one reported in the present work, has been carried out also on other polycrystalline samples with different doping. The results obtained show that no substantial difference exists with the results reported in this paper, at least when the detection and the behavior of the different flux dynamics regimes is concerned. In particular, no clear indication of a possible correlation between the vortex dynamics and the oxygen content has been found. However, the availability of good quality single crystals, with different doping levels, is needed to investigate the complete vortex phase diagram and to infer possible effects related to the different doping.

ACKNOWLEDGMENTS

We kindly thank A. Vecchione and R. Fittipaldi for useful and fruitful discussions.

*Corresponding author. FAX: +39089965275; polimax@fisica.unisa.it

[1] Y. Kamihara, T. Watanabe, M. Hirano, and H. Hosono, J. Am. Chem. Soc. **130**, 3296 (2008).

[2] J. G. Bednorz and K. A. Muller, Z. Phys. B: Condens. Matter **64**, 189 (1986).

[3] A. F. Hebard, M. J. Rosseinsky, R. C. Haddon, D. W. Murphy, S. H. Glarum, T. T. M. Palstra, A. P. Ramirez, and A. R. Kortan, Nature (London) **350**, 600 (1991).

[4] J. Nagamatsu, N. Nakagawa, T. Muranaka, Y. Zenitani, and J. Akimitsu, Nature (London) **410**, 63 (2001).

[5] T. Watanabe, H. Yanagi, T. Kamiya, Y. Kamihara, H. Hiramatsu, M. Hirano, and H. Hosono, Inorg. Chem. **46**, 7719 (2007).

[6] B. I. Zimmer, W. Jeitschko, J. H. Albering, R. Glaum, and M.

Reehuis, J. Alloys Compd. **229**, 238 (1995); P. Quebe, L. J. Terbüchte, and W. Jeitschko, *ibid.* **302**, 70 (2000).
[7] V. Johnson and W. Jeitschko, J. Solid State Chem. **11**, 161 (1974).
[8] D. J. Singh and M. H. Du, Phys. Rev. Lett. **100**, 237003 (2008).
[9] A. S. Sefat, M. A. McGuire, B. C. Sales, R. Jin, J. Y. Howe, and D. Mandrus, Phys. Rev. B **77**, 174503 (2008).
[10] G. F. Chen, Z. Li, G. Li, J. Zhou, D. Wu, J. Dong, W. Z. Hu, P. Zheng, Z. J. Chen, H. Q. Yuan, J. Singleton, J. L. Luo, and N. L. Wang, Phys. Rev. Lett. **101**, 057007 (2008).
[11] C. de la Cruz, Q. Huang, J. W. Lynn, W. Jiying Li, I. I. Ratcliff, J. L. Zarestky, H. A. Mook, G. F. Chen, J. L. Luo, N. L. Wang, and Pengcheng Dai, Nature (London) **453**, 899 (2008).
[12] M. Tinkham, *Introduction to Superconductivity* (McGraw-Hill, New York, 1997).
[13] F. Gomory, Supercond. Sci. Technol. **10**, 523 (1997), and references therein.
[14] X. Ling and J. I. Budnick, in *Magnetic Susceptibility of Superconductors and Other Spin Systems*, edited by R. A. Hein, T. L. Francavilla, and D. H. Liebenberg (Plenum, New York, 1991), pp. 377–388, and references therein.
[15] D. Di Gioacchino, F. Celani, P. Tripodi, A. M. Testa, and S. Pace, Phys. Rev. B **59**, 11539 (1999).
[16] M. Polichetti, M. G. Adesso, and S. Pace, Eur. Phys. J. B **36**, 27 (2003).
[17] M. J. Qin and C. K. Ong, Phys. Rev. B **61**, 9786 (2000).
[18] M. Polichetti, M. G. Adesso, T. Di Matteo, A. Vecchione, and S. Pace, Physica C **332**, 378 (2000).
[19] M. G. Adesso, C. Senatore, M. Polichetti, and S. Pace, Physica C **404**, 289 (2004).
[20] M. G. Adesso, M. Polichetti, and S. Pace, Physica C **401**, 196 (2004).
[21] M. G. Adesso, D. Uglietti, R. Flükiger, M. Polichetti, and S. Pace, Phys. Rev. B **73**, 092513 (2006).
[22] A. Martinelli, M. Ferretti, P. Manfrinetti, A. Palenzona, M. Tropeano, M. R. Cimberle, C. Ferdeghini, R. Valle, C. Bernini, M. Putti, and A. S. Siri, Supercond. Sci. Technol. **21**, 095017 (2008).
[23] A. Yamamoto, J. Jiang, C. Tarantini, N. Craig, A. A. Polyanskii, F. Kametani, F. Hunte, J. Jaroszynski, E. E. Hellstrom, D. C. Larbalestier, R. Jin, A. S. Sefat, M. A. McGuire, B. C. Sales, D. K. Christen, and D. Mandrus, Appl. Phys. Lett. **92**, 252501 (2008).
[24] J. R. Clem, Physica C **153-155**, 50 (1988).
[25] Th. Herzog, H. A. Radovan, P. Ziemann, and E. H. Brandt, Phys. Rev. B **56**, 2871 (1997).
[26] A. V. Silhanek, S. Raedts, and V. V. Moshchalkov, Phys. Rev. B **70**, 144504 (2004).
[27] H. M. Jaeger, D. B. Haviland, B. G. Orr, and A. M. Goldman, Phys. Rev. B **40**, 182 (1989).
[28] D.-X. Chen, E. Pardo, A. Sanchez, and E. Bartolomé, Appl. Phys. Lett. **89**, 072501 (2006).
[29] O. Ozogul, Phys. Status Solidi A **202**, 1793 (2005).
[30] C. P. Bean, Phys. Rev. Lett. **8**, 250 (1962).
[31] M. G. Adesso, Ph.D. thesis, Università di Salerno, 2005.
[32] D. Di Gioachino, A. M. Testa, S. Pace, P. Tripodi, and F. Celani, Philos. Mag. B **80**, 997 (2000).
[33] M. G. Adesso, M. Polichetti, and S. Pace, J. Phys.: Condens. Matter **20**, 385211 (2008).